RIVER RESEARCH AND APPLICATIONS
River Res. Applic. **28**: 377–389 (2012)
Published online 18 October 2010 in Wiley Online Library
(wileyonlinelibrary.com) DOI: 10.1002/rra.1463

FLOW STRUCTURE THROUGH POOL-RIFFLE SEQUENCES AND A CONCEPTUAL MODEL FOR THEIR SUSTAINABILITY IN GRAVEL-BED RIVERS

D. CAAMAÑO,[a*] P. GOODWIN[b] and J. M. BUFFINGTON[c]

[a] *Centro EULA-Chile, Universidad de Concepción, Barrio Universitario s/n, Concepción, Chile*
[b] *Center for Ecohydraulics Research, University of Idaho, Boise, Idaho 83702, USA*
[c] *Rocky Mountain Research Station, U.S. Forest Service, Boise, Idaho 83702, USA*

ABSTRACT

Detailed field measurements and simulations of three-dimensional flow structure were used to develop a conceptual model to explain the sustainability of self-formed pool-riffle sequences in gravel-bed rivers. The analysis was conducted at the Red River Wildlife Management Area in Idaho, USA, and enabled characterization of the flow structure through two consecutive pool-riffle sequences, including: identification of jet concentration and dissipation zones, and the development of local turbulence features (i.e. vertical and horizontal eddies) under different flow conditions. Three-dimensional hydraulic simulations were used to evaluate how the flow structure varies across a range of flow conditions and with different degrees of sediment aggradation within the upstream pool. The analysis demonstrated a significant influence of the residual pool depth on the flow structure, with reduced residual depth causing a shift in the orientation of the jet and a reduction in the influence of vertical eddies and the size and intensity of horizontal eddies. The proposed conceptual model seeks to explain the sustainability of pools in terms of the flow structure in pool-riffle morphology and how this flow structure will change as a result of altered external forcing, such as upstream sediment delivery or changes in bank stability.

KEY WORDS: Gravel-bed rivers; pools; riffles; 3-d models; Red River; ADCP measurements; MIKE 3 FM

Received 16 April 2010; Accepted 23 August 2010

INTRODUCTION

Velocity reversal has been hypothesized as a mechanism for the sustainability of pool morphology in gravel-bed rivers (e.g. Gilbert, 1914, Keller, 1971, Lisle, 1979), and recent studies have shown that cross-sectional average velocity reversal will occur under certain bathymetric and flow conditions (Caamaño *et al*., 2009). However, cross-sectional average parameters do not capture the spatial variability of the three-dimensional flow within pool-riffle sequences. Consequently, conclusions regarding velocity reversal as a mechanism for the sustainability of pool morphology may be influenced by the simplifications introduced by a one-dimensional approximation.

As a first step towards addressing this problem, a detailed analysis of the three-dimensional flow structure was conducted in two consecutive pool-riffle sequences in the Red River Wildlife Management Area, north-central Idaho, USA. The study reach is located immediately downstream of a restoration project that was implemented in the period 1998–2001 and monitored annually (Klein *et al*., 2007). The selected pool-riffle sequences formed shortly after completion of the restoration project, and are among the deepest pools in the meadow. These two pool-riffle sequences have persisted in time while other pools in the meadow have disappeared. The focus of this study is to describe the pool-riffle flow structure and to relate it to the sustainability of this morphology. The flow structure was measured in the field at three different discharges and also characterized by three-dimensional hydraulic modelling. Model results show good agreement with the measured water surface elevations (WSE) and velocities. Similar trends and complementary conclusions to those found by Booker *et al*. (2001), MacWilliams *et al*. (2006), Harrison and Keller (2007) and MacVicar and Roy (2007) are shown here.

Flow jets (i.e. concentration of high flow velocities) are observed at all discharges in this study and are characterized for different flow and pool bathymetry conditions. The magnitude, shape and location of the jets change according to the flow and residual pool depth values (Lisle, 1987). The bathymetry creates the jet, but the strength of the jet generates local turbulent features that, in turn, likely sustain the bathymetry. These local eddies influence the shear stresses and erosion potential along the banks and channel bed. Deep pools exhibit stronger vertical turbulence features close to the thalweg, with jets aligned through the shallower part of their cross sections. Conversely, shallow pools (due to sediment deposition) tend to have less pronounced vertical turbulence structure close to the thalweg and are

*Correspondence to: D. Caamaño, Centro EULA-Chile, Universidad de Concepción, Barrio Universitario s/n, Concepción, Chile.
E-mail: dcaamano@udec.cl

characterized by jets that flow through the deeper parts of the channel cross sections. Using a detailed description of the predicted flow structure, the study identifies and proposes a conceptual model based on jet concentration and dissipation zones. The proposed conceptual model aids in understanding the physical processes of pool-riffle sustainability due to local changes in the flow structure and external factors that alter sediment supply and or hydrology.

THE STUDY SITE

Red River is located in north-central Idaho (lat. 45° 45’, long. 115° 24’), USA. The study reach is a meandering gravel-bed channel that flows through an unconfined 4.5 km long meadow situated at an elevation of 1280 m and bounded by forested mountains that reach 2134 m (Klein *et al*., 2007) (Figure 1). The two selected pool-riffle sequences are free formed (not forced by external flow obstructions such as logs or boulders; Montgomery *et al*., 1995) and are situated downstream of a straight, 50 m long run. The channel curves into a double pool-riffle sequence with a bank top width of 11.25 m, and then opens to a wider stream. The upstream run has a symmetrical, almost rectangular cross section that allows a uniform flow distribution in the stream before entering the first pool.

The first pool-riffle sequence has a deep residual pool depth followed by a coarse riffle, whereas the second pool is shallower, with a finer-grained riffle (Table I). A calibrated 1-dimensional hydraulic model was used to simulate flow conditions through the entire meadow (MIKE 11 developed by the DHI, Denmark), within which a 150 m reach of the river was considered for detailed three-dimensional modelling, with the pool-riffle sequences of interest covering a channel length of 45 m within this reach.

Figure 1. Location of the pool-riffle sequences within the Red River study site. This figure is available in colour online at wileyonlinelibrary.com

Table I. Grain size distribution

Bedforms	d_{16} (*mm*)	d_{50} (*mm*)	d_{84} (*mm*)	d_{90} (*mm*)
Pool 1	12	42	74	82
Riffle 1	38	65	94	105
Pool 2	19	46	82	90
Riffle 2	26	47	80	85

FIELD MEASUREMENTS

The primary data used in the flow modelling include channel topography, grain size and a measured stage-discharge relationship at the downstream boundary of the numerical domain. Field measurements of WSE and the velocity structure at a known discharge were used for model calibration. Channel topography was surveyed using a Leica Real-Time Kinematic Global Positioning System (RTK GPS), with a horizontal and vertical accuracy of 10 and 20 mm, respectively (Figure 2). About 6400 points were taken to represent the study area, with a higher point density within the pool-riffle zones (about 8 points/m^2). The bathymetry was obtained from a point-based Triangulated Irregular Network (TIN; Figure 3). Grain size was determined using Wolman (1954) pebble counts conducted within each pool and riffle (Table I), supplemented by particle size distributions of bed samples taken throughout the Red River Wildlife Management Area for parameterizing the channel roughness. Three different discharge scenarios were measured and assessed in this study, 0.38, 5.67 and 9.23 m^3/s which corresponded to a typical summer low flow, an intermediate flow and high-flow event, respectively (Figure 4). A fourth discharge corresponding to bankfull (16.63 m^3/s; Klein *et al*., 2007) was included in the modelling to cover the complete range of instream flows. Both bathymetry and grain-size information were collected during the low-flow event.

A Sontek handheld Acoustic Doppler Velocimeter (ADV) and RDI StreamPro Acoustic Doppler Current Profiler (ADCP) were used to measure discharge and 1 min average vertical velocity profiles. The ADV worked better than the ADCP for water depths shallower than 20 cm and, therefore, was the instrument used for all sampling during the low-flow event (the only sampled discharge for which it was feasible to wade the stream). The ADCP was used for the two higher events, with the ADV being used only near the banks in the shallow parts of the flow. The StreamPro ADCP measures

DOI: 10.1002/rra

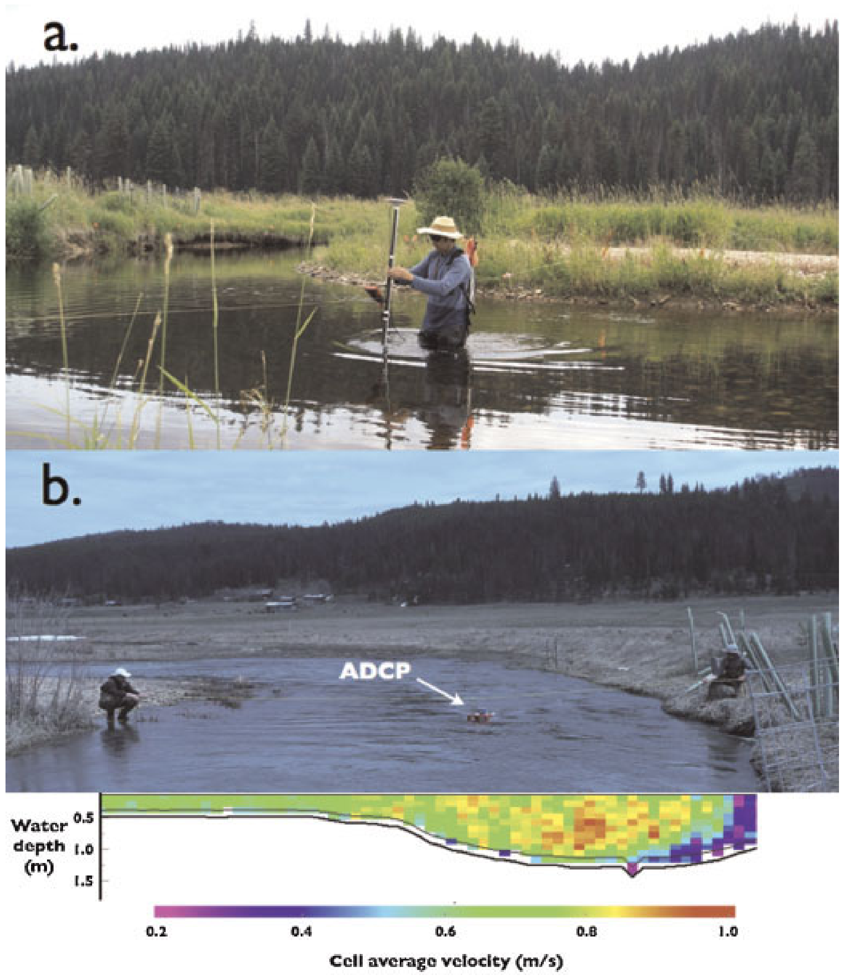

Figure 2. Measuring devices used in this study: a) GPS rover (bathymetry, water depth, and water surface elevation) and b) StreamPro ADCP (discharge and vertical velocity profiles). The velocity distribution is shown high (red) to low (purple). This figure is available in colour online at wileyonlinelibrary.com

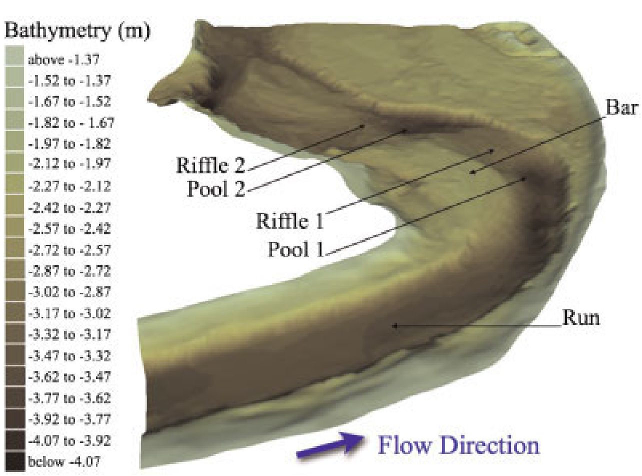

Figure 3. Study site topography, showing the locations of the pool-riffle-sequences. This figure is available in colour online at wileyonlinelibrary.com

discharge and characterizes the velocity profile with a range of 1 to 20 vertical cells, with a minimum and maximum cell size of 2 and 10 cm, respectively (Figure 2b). Discharge was measured at 3 cross sections, with measurements repeated four times per cross section to obtain an average value that had less than 5% error between measurements. The velocity structure was also measured for each of the four discharge measurements. WSE throughout the pool-riffle sequences were obtained for each flow scenario. At low flow, water depths were recorded using a measuring tape attached to the GPS rod when surveying the bathymetry. A total of 40 points were measured within the 150 m model domain. At higher flows, the edge-of-water elevations were recorded and were supplemented by additional depth measurements wherever the flow conditions were safe to be in the stream. A total of 35 points at the low flow (5.67 m^3/s) and 47 points at the high flow (9.23 m^3/s) were obtained.

DOI: 10.1002/rra

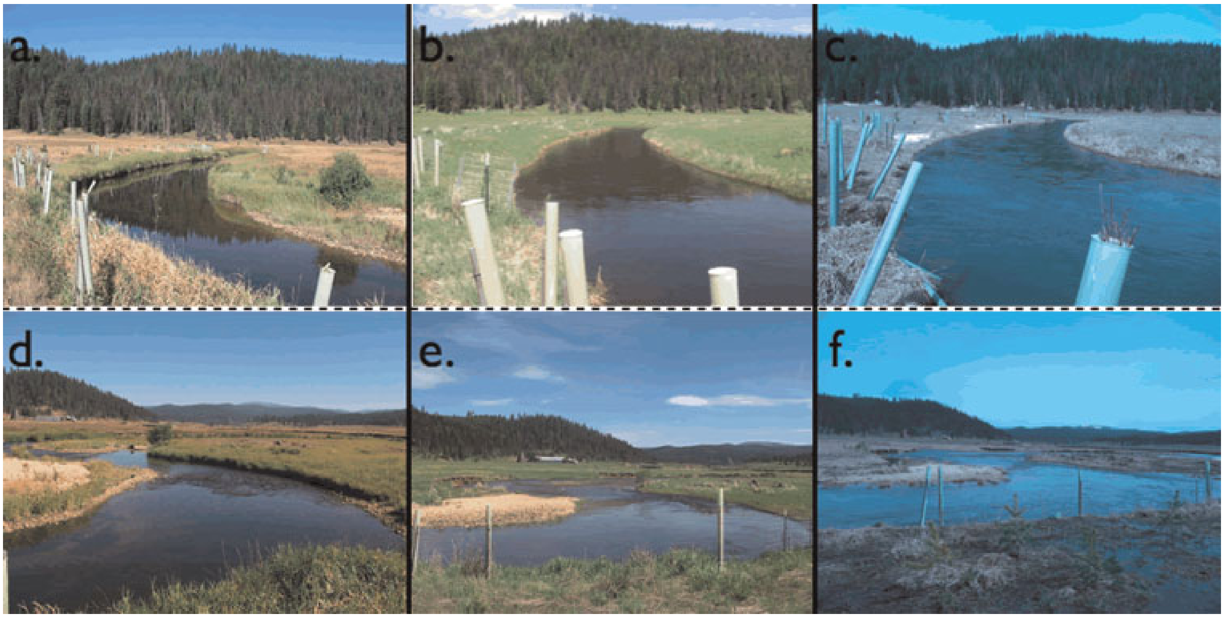

Figure 4. Photographs of the upstream run (a–c) and the first pool-riffle sequence (d–f) for the three discharge scenarios (0.38, 5.67 and 9.23 m^3/s, respectively). This figure is available in colour online at wileyonlinelibrary.com

NUMERICAL SIMULATIONS

The MIKE 3 Flexible Mesh (FM) program was used in this study to characterize the pool-riffle flow structure. Developed by DHI (Denmark), it is based on the three-dimensional incompressible Reynolds-average Navier-Stokes equations, subject to the assumptions of the Boussinesq approximation and hydrostatic pressure (DHI, 2008). The model uses a comprehensive set of equations to describe the hydrodynamics. The system of equations used in this study is described by Caamaño (2008). It was assumed that infiltration at the sediment–water interface (i.e. hyporheic exchange) and flux at the water surface (i.e. precipitation/evaporation) are negligible, with water entering or leaving the model domain only at the upstream and downstream cross sections. This was considered a reasonable assumption, as there was no detectable difference in the discharge at the upstream and downstream boundaries of the study reach during each flow event.

For turbulent closure, the model uses a vertical k-ε eddy viscosity (Rodi, 1984) and a horizontal Smagorinsky, subgrid scale, eddy viscosity (Smagorinsky, 1963). The spatial discretization of the equations is performed using a cell-centered finite volume method. The spatial domain is discretized by subdivision of the continuum into non-overlapping elements/cells. In the horizontal plane a triangular unstructured grid is used, while in the vertical domain a structured mesh is considered (DHI, 2008). These equations are solved using a vertical σ-transformation (Phillips, 1957).

Mesh sensitivity analysis was conducted for mesh sizes from 1 to 0.06 m^2, and the results were shown to be independent from the spatial discretization for element areas of 0.075 m^2 and less. Thus, the modelled area was covered with a total of 33 258 unstructured equilateral triangular elements by 10 structured vertical layers (332 580 three-dimensional elements). A wet-cell criterion with a minimum depth of 2 cm was imposed for inclusion of cells within the solution domain.

The bottom stress is determined by a quadratic friction law ($\tau_b = \rho c_f u_b^2$) based on the water density (ρ), the drag coefficient (c_f), and the flow velocity near the bed (u_b). The drag coefficients are calculated by assuming a logarithmic profile between the river bed and a point located at 10% of the water depth from the bottom (Δz)

$$c_f = \left(\frac{K}{\ln\left(\frac{\Delta z}{z_0}\right)} \right)^2 \quad (1)$$

where $K = 0.4$ is the von Kármán constant and $z_0 = m \times d_{84}$ is the bed roughness length scale with the constant $m = 0.065$ obtained by model calibration. A logarithmic profile is unrealistic for low values of relative submergence (depth divided by grain size), which becomes an issue for boulder-bed channels and gravel-bed channels at low flow (Wiberg and Smith, 1991, Lamb *et al.*, 2008), where the hydrostatic assumption also breaks down. However, low flow is used here only as a reference scenario, given that the flow structure, from the point of view of pool-riffle sustainability,

DOI: 10.1002/rra

will be relevant only at medium to high flows, for which the hydrostatic assumption is realistic, provided that the bedforms are submerged (Tonina and Buffington, 2007).

The boundary conditions for the model are specified as an upstream discharge and a downstream water surface elevation. The discharge is distributed uniformly across the upstream boundary condition, allowed by the symmetrical cross section and the length of the upstream run; detailed measurements taken with the ADCP and ADV verified that this assumption was reasonable (Caamaño, 2008). The downstream water surface elevation was based on field measurements and compared with a stage–discharge relationship developed from the MIKE 11 one-dimensional model of the entire Red River Meadow. The location of the downstream boundary (approximately 50 m downstream from the second pool-riffle sequence) was selected as a balance between minimizing the extent of the three-dimensional model domain, to reduce computational run time, but far enough downstream that any errors generated at the downstream boundary do not propagate at a significant level into the region of interest. Several water surface measurements were taken across the selected downstream boundary section, demonstrating a fairly horizontal water level (Caamaño, 2008), and suggesting that the downstream boundary condition can be approximated by a single value.

Model calibration was performed using WSE and velocities for all three observed discharges. Currently the RDI StreamPro ADCP does not include a compass, so although reasonable cross-sectional profiles of the three-dimensional velocity components are obtained, the precise orientation of the local velocity components at any point in the cross-section is not known. To the authors' knowledge the technology is not yet available to characterize the precise directionality of the three-dimensional velocity structure in shallow streams like our study site (see review by Gunawan *et al*., 2009). However, the ability to measure and visualize the three-dimensional flow structure in a relative sense in the field under flood conditions is a major step forward. The overall flow structure measured in the field is representative of reality, but makes accurate calibration of velocity direction difficult (i.e. all three velocity directions). Therefore, the model was calibrated by comparing the velocity magnitude given by $\sqrt{u^2 + v^2 + w^2}$ (where u, v, w are the time-average velocity components in the x, y, z directions) at points along the vertical velocity profiles. Root mean square errors (RMSE) between measured and predicted values of WSE are shown in Table II and individual points are plotted in Figure 5. Predicted and measured velocities were compared at several locations in the main channel and an example of these comparisons in the regions of interest at high discharge is shown in Figure 6. Despite some minor discrepancies between the observed and modelled values (average RMSE of 0.08 m/s), the model does replicate the velocity profiles for all three flow scenarios.

Table II. RMSE for measured and predicted water surface elevations

Discharge (m^3/s)	Number of points	RMSE (*m*)
0.38	40	0.020
5.67	35	0.021
9.23	47	0.026

Furthermore, the computed velocity profiles captured the non-logarithmic characteristics of the velocity profiles measured in the field.

IDENTIFICATION OF PRINCIPAL FLOW FEATURES

Similar to prior studies (e.g. Dietrich and Smith, 1983, 1984), the observations and model results indicate that the fast-moving water is confined to a portion of the cross-sectional area in the pools, whereas the fast-moving flow in the riffles is distributed throughout most of the cross section (Figure 7). This region of concentrated fast-moving water was observed by MacWilliams *et al*. (2006), and is the basis for their ''flow routing hypothesis''. Their study proposes that an upstream flow constriction will result in a convergence and acceleration of flow at the head of the pool, which generates a jet of flow through and downstream of the constriction. This zone of high velocity produces high shear stress, and represents the primary pathway for sediment movement through the pool (MacWilliams *et al*., 2006). The flow routing hypothesis is therefore based on the concentrated fast-moving portion of the flow that was identified as a flow jet. However, the MacWilliams *et al*. (2006) approach lacks a jet

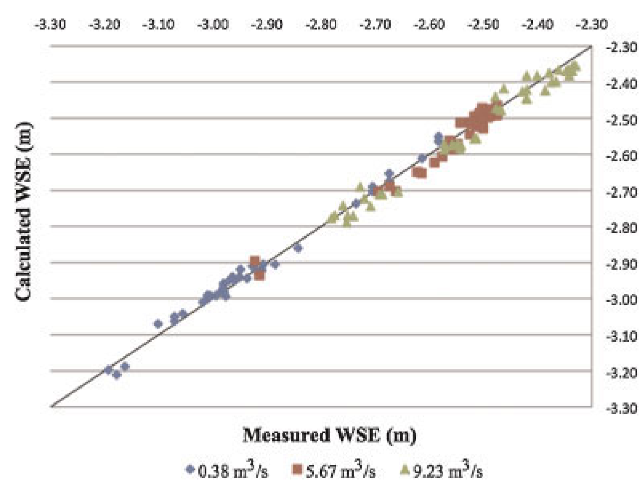

Figure 5. Calibration of observed and calculated WSE. This figure is available in colour online at wileyonlinelibrary.com

DOI: 10.1002/rra

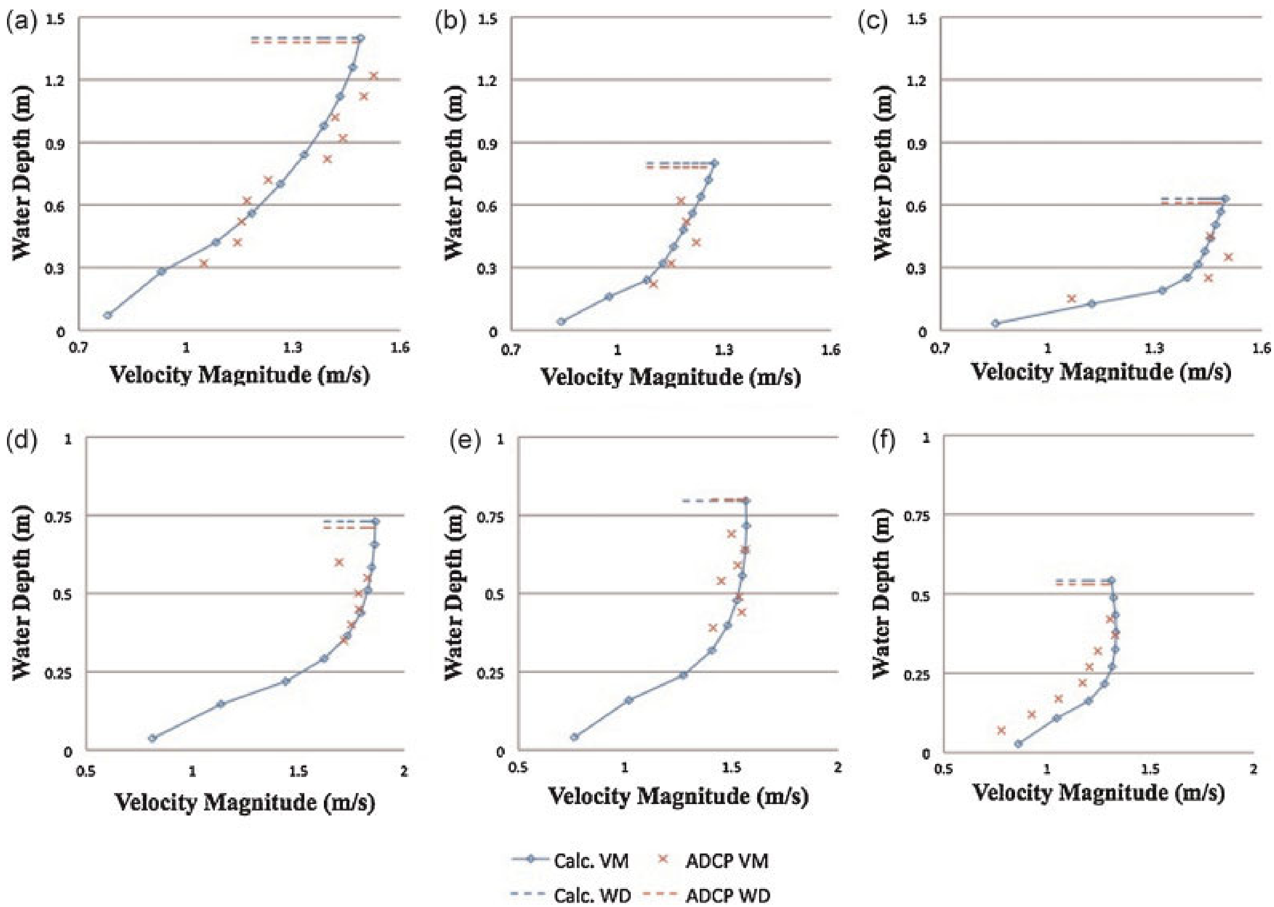

Figure 6. Observed (ADCP) and calculated velocity magnitudes (VM) and water depths (WD) after calibration within concentrated flow areas (jets) during the 9.23 m^3/s event: a) Upstream pool, b) Upstream pool tail, c) Upstream riffle, d) Downstream pool head, e) Downstream pool and f) Downstream riffle. This figure is available in colour online at wileyonlinelibrary.com

definition, and thus it is not possible to characterize the jet under different scenarios except to note its existence. In order to analyze the jet and the associated pool-riffle flow structure, the present study defines the jet as formed by velocities that are higher than 90% of the maximum depth-averaged velocity observed within a reference cross section (defined here as the cross section traversing the deepest portion of the upstream pool). This definition best showed the spatial pattern and limits (i.e. edges) of the jet over the range of flows studied.

Flow structure under existing bathymetric conditions

The spatial pattern of the jets is visualized in Figure 8 in terms of time-averaged surface velocities predicted from the numerical model. Jets were found to be present at all three flow scenarios that were observed in the field and simulated in the model. Large-scale turbulence features, such as vertical and horizontal eddies, did not occur in the jet flow, but were observed outside the region delineating the jets.

Low flow (Figure 8a). Pool 1: The point bar created a zone of flow contraction at the head of the pool as water accelerates into it, defining a zone of jet concentration (Jet 1). As the channel width increases from the pool towards the riffle, the jet also increases in width as more slower moving water is entrained. This area is defined as a zone of jet dissipation. High velocities were observed at the centre of the run cross sections, but as the flow moves downstream, the jet moves towards the inner bank, resulting in higher velocities over the bar than along the pool thalweg at the tail of the pool (Booker *et al*., 2001, MacWilliams *et al*., 2006, Harrison and Keller, 2007). As the flow exits the pool, it becomes more evenly distributed across the riffle, after which higher velocities developed downstream of the riffle crest as the flow concentrates towards the second pool. Considering that surface velocities are related to near-bed flow conditions, except in areas of eddies or stratified flow, it is not surprising to observe higher near-bed velocities across the bar, especially upstream of the apex of the bend, where the velocity gradient is stronger (Figure 9a). There is a zone of separation along the edge of the deepest portion of the

DOI: 10.1002/rra

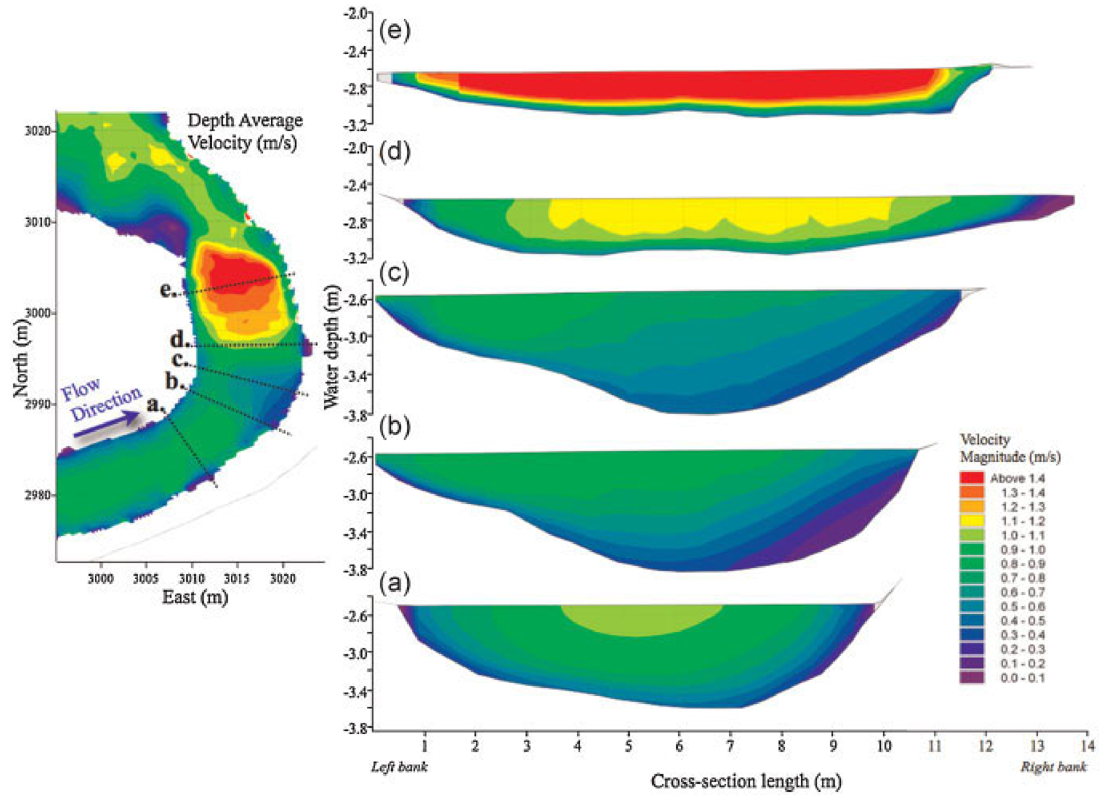

Figure 7. Cross-sectional distribution of velocity, showing a more uniform distribution in the upstream run (a) and downstream riffle (d, e) than within the pool (b, c). This figure is available in colour online at wileyonlinelibrary.com

pool that influences the secondary current direction and is also an area where vertical eddies are formed at higher flows (Figures 8 and 9). The location of the eddy corresponds with a narrowing (i.e. concentration) of the jet (Figure 8a).

Pool 2: A similar pattern of jet concentration and dissipation is observed at the downstream pool and characterized by a second jet (Jet 2). Jet concentration occurs as the flow constricts from the upstream riffle into the

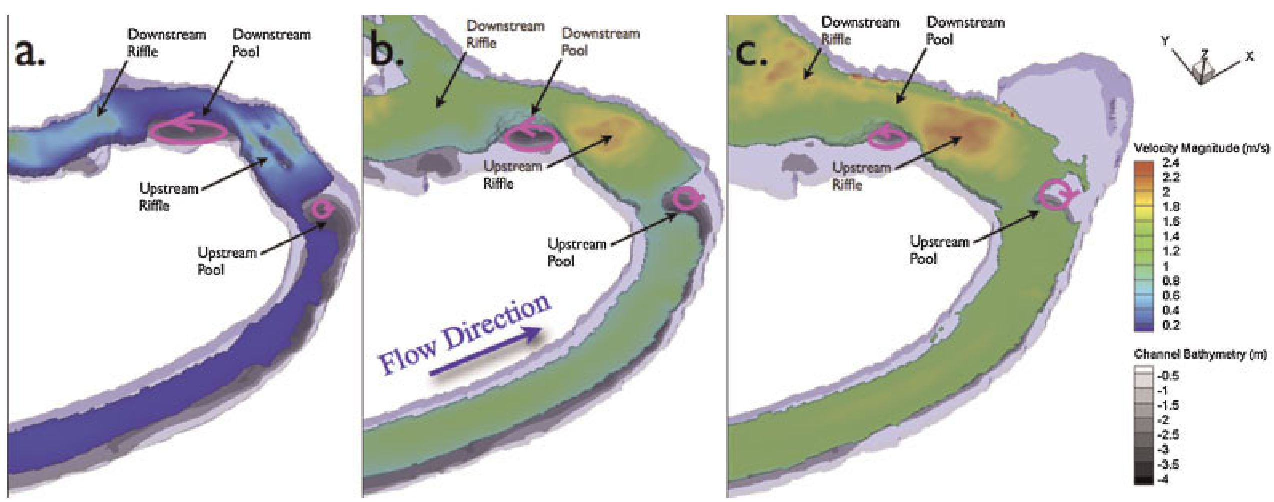

Figure 8. Predicted jet patterns and time-averaged surface velocities. Jets are represented by the entire coloured area of the flow in each panel, with the wetted bathymetry shown by grey shading: a) low flow (0.38 m3/s), b) medium flow (5.67 m3/s), and c) high flow (9.23 m3/s). Jet velocities are defined as > 0.09, 0.7, and 1 m/s, respectively, using the 90% criterion (see text). Circular arrows (outer bank) indicate vertical eddies, and elliptical ones (inner bank) indicate horizontal eddies. This figure is available in colour online at wileyonlinelibrary.com

DOI: 10.1002/rra

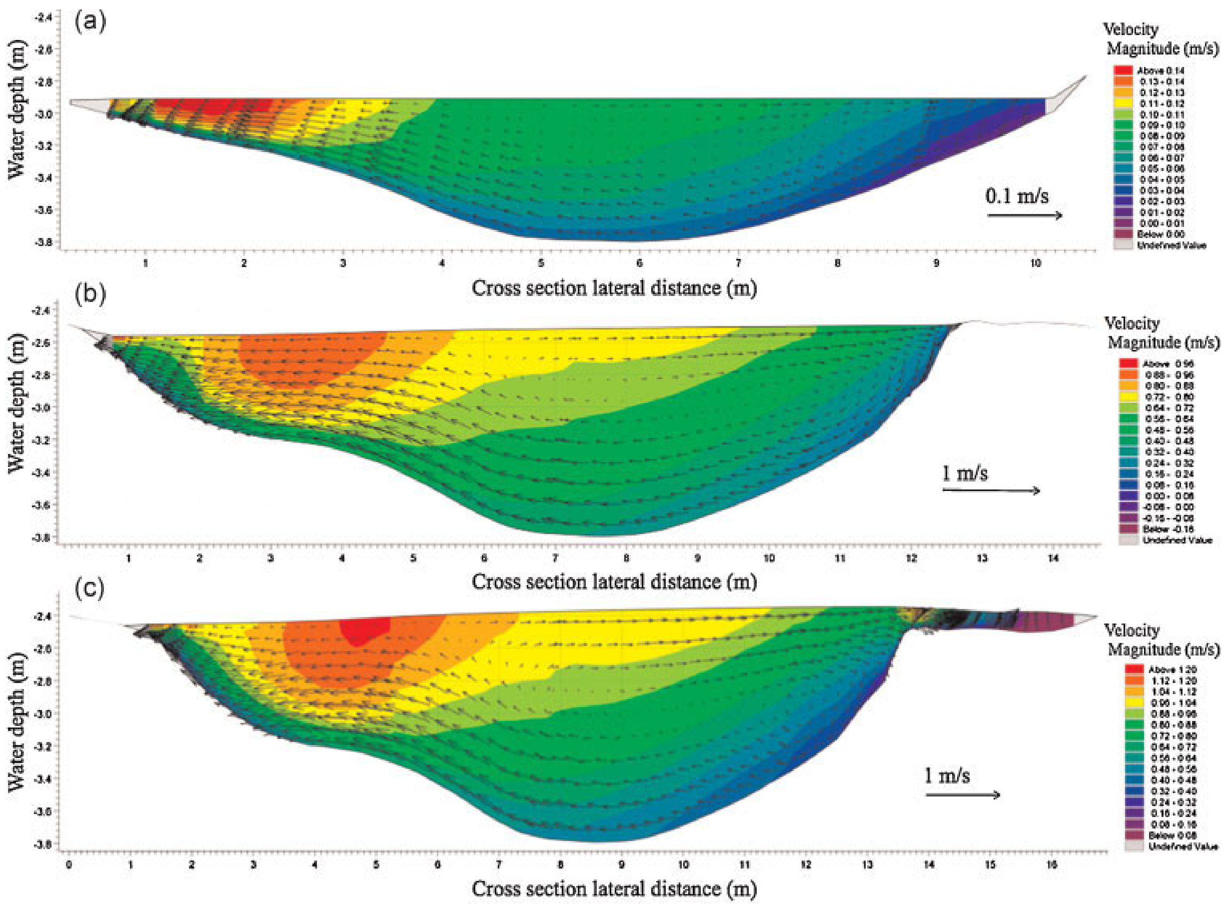

Figure 9. Predicted lateral velocity distribution for the upstream pool during discharges of: a) 0.38, b) 5.67 and c) 9.23 m^3/s. Vectors indicate patterns of secondary circulation. Note that the horizontal scale and the range of velocity magnitudes increase with discharge. This figure is available in colour online at wileyonlinelibrary.com

pool, with the jet remaining close to the outer bank and through the deepest part of the pool before expanding into a more uniformly distributed velocity across the associated downstream riffle. Jet 2 was longer than Jet 1. A horizontal eddy is sustained by Jet 2 on the inner bank just downstream of the first riffle (downstream elliptical arrow in Figure 8a), with the eddy causing constriction and concentration of the jet.

Intermediate flow (Figure 8b). Pool 1: At intermediate flow, strong, large, vertical, turbulence structures are observed in the deepest portion of the pool (upstream circular arrow in Figure 8b, and correspond with concentration of the jet). The vertical eddies maintained their position at about 50–60% of the water depth (Figure 9b). They exist at the deepest part of the pool, towards the outer bank and opposite to the location of Jet 1. The location of the vertical eddies coincides with the point where the lateral current changes direction towards the outer bank on its way to the surface from the channel bed (Figure 9b). This is consistent with observations made by Dietrich and Smith (1984).

Pool 2: The length of Jet 2 was conserved with increasing discharge as it is constrained by the two riffles. The horizontal eddy persisted along the inner bank, however it moved upstream, decreased its diameter and increased its core velocity with discharge. The jet narrows along the horizontal eddy, but expands with increasing discharge as the eddy decreases in diameter.

High flow (Figure 8c). Pool 1: With increasing discharge, Jet 1 gets wider, shorter and faster than the jet observed at low flow. The jet increased its width to cover a portion of the deeper area of the pool. At this flow, water spilled onto the floodplain along the right bank, and the vertical eddies increased in magnitude.

Pool 2: The horizontal eddy moved further upstream, decreased in size and increased its core velocity with discharge. In contrast with the vertical eddies of the upstream pool, this horizontal turbulence feature was observed throughout the entire water column at all discharges. The angle of growth of the width of the jet increased as the diameter of the eddy decreased due to the shear zone generated on the interface between the rapid and slow fluid motion (Jirka, 2007).

DOI: 10.1002/rra

Effect of upstream pool infilling on flow structure

The potential influence of sediment aggradation on the flow structure of the study reach was investigated for two simulated cases in which the residual depth of the upstream pool was reduced by (a) 30% and (b) 90%. For the purposes of this evaluation and in the absence of field data of deposition patterns, it was assumed that deposition was horizontal throughout the pool. The simulations were conducted for the high flow condition (9.23 m^3/s) and for bankfull discharge (16.63 m^3/s), which may be particularly relevant for pool maintenance, both in terms of the dominant (Wolman and Miller, 1960) or effective discharge (Goodwin, 2004) and velocity reversal (e.g. Keller, 1971, Lisle, 1979, Caamaño *et al*., 2009).

Results show changes in the flow structure of the upstream pool-riffle sequence, but very little change in the downstream one, suggesting that the downstream riffle acts as a hydraulic control (Figure 10). A 30% shallowing of the residual depth in the upstream pool caused the Jet 1 core velocities to increase, and the upstream pool showed weaker vertical turbulence structures on the right bank of the pool with decreasing water depths (Figure 11). In contrast, 90% filling of the upstream pool created a more symmetrical cross section that did not develop significant vertical turbulence structures on the right bank, but instead created a well-defined vertical eddy on the left bank (Figure 11c).

High velocities still occurred near the surface within the infilled pool, however changes in the lateral velocity distribution were observed in response to the simulated aggradation (Figures 10 and 11). For a 30% reduction of the residual pool depth, Jet 1 did not change its lateral position, but velocities increased in the central part of the cross section, making Jet 1 wider (Figures 10 and 11). Jet velocities kept increasing with filling, and at 90%, there was a significant realignment of Jet 1 that directed it towards the outer bank. The jet was considerably wider with this amount of aggradation and had a greater impact on the banks.

Secondary flow structure and movement of the jet

The relationship between the lateral water surface slope and secondary circulation is shown for the upstream pool, with greater discharges producing a larger cross-channel slope and greater helical flux of outward moving surface water and inward moving flow near the bed (Figure 9). A simple interpretation of the energy equation would imply that pool sections with low velocities and large depths should establish a lateral pressure gradient towards the shallow, higher-velocity flows across the bar, similar to that discussed by Dietrich *et al*. (1979). This lateral pressure gradient forces the jet to flow across the bar on the inside of the bend at low and intermediate discharges, which is further reinforced by the Coanda effect (Tritton, 1977). Figure 9a–c show the position of the jet as a function of discharge at the cross section in the deepest portion of the upstream pool. The pressure gradient guides the jet towards the inner bank at low flows, but the jet is moved back towards the pool thalweg at high flows as the longitudinal momentum becomes more dominant and as the flow is forced to shoal over the bar (Dietrich *et al*., 1979, Dietrich and Smith, 1983). The effects of pool infilling due to sedimentation are also shown (Figure 11). As the pool residual depth decreases, the tendency for the jet to flow across the bar at low and intermediate flows is less pronounced and the jet persists more within the centre of the pool. The different alignment of the jet at different discharges is proposed in this study as an important mechanism for pool-riffle sustainability.

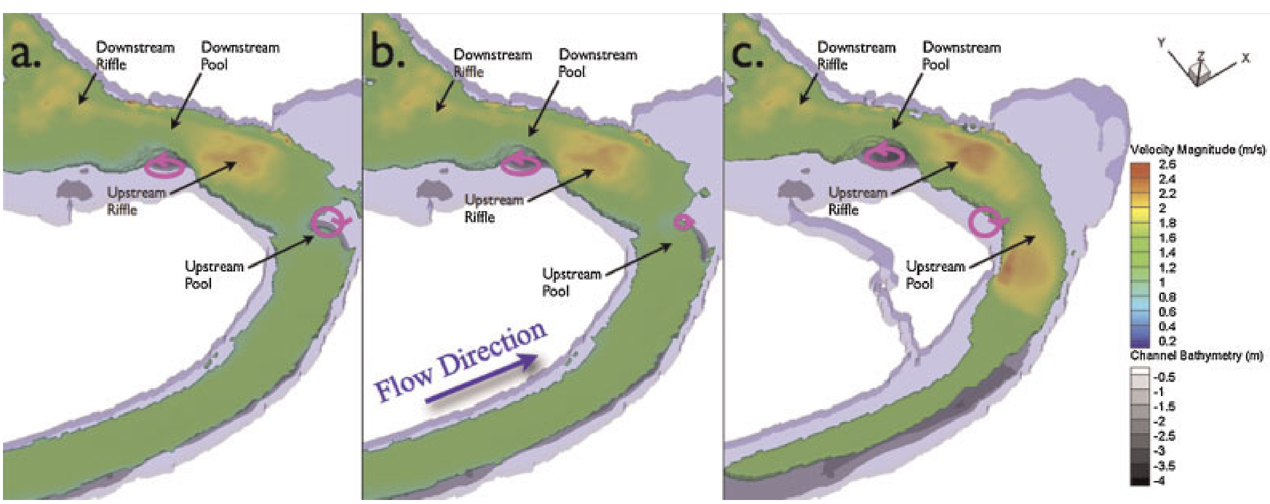

Figure 10. Predicted jet patterns and time averaged surface velocities for the 9.23 m^3/s flow for: a) original topography, b) 30% aggradation of residual depth in the upstream pool and c) 90% aggradation of the same pool. Jet velocities are defined as 1.00, 1.05 and 1.24 m/s, respectively, using the 90% criterion (see text). This figure is available in colour online at wileyonlinelibrary.com

DOI: 10.1002/rra

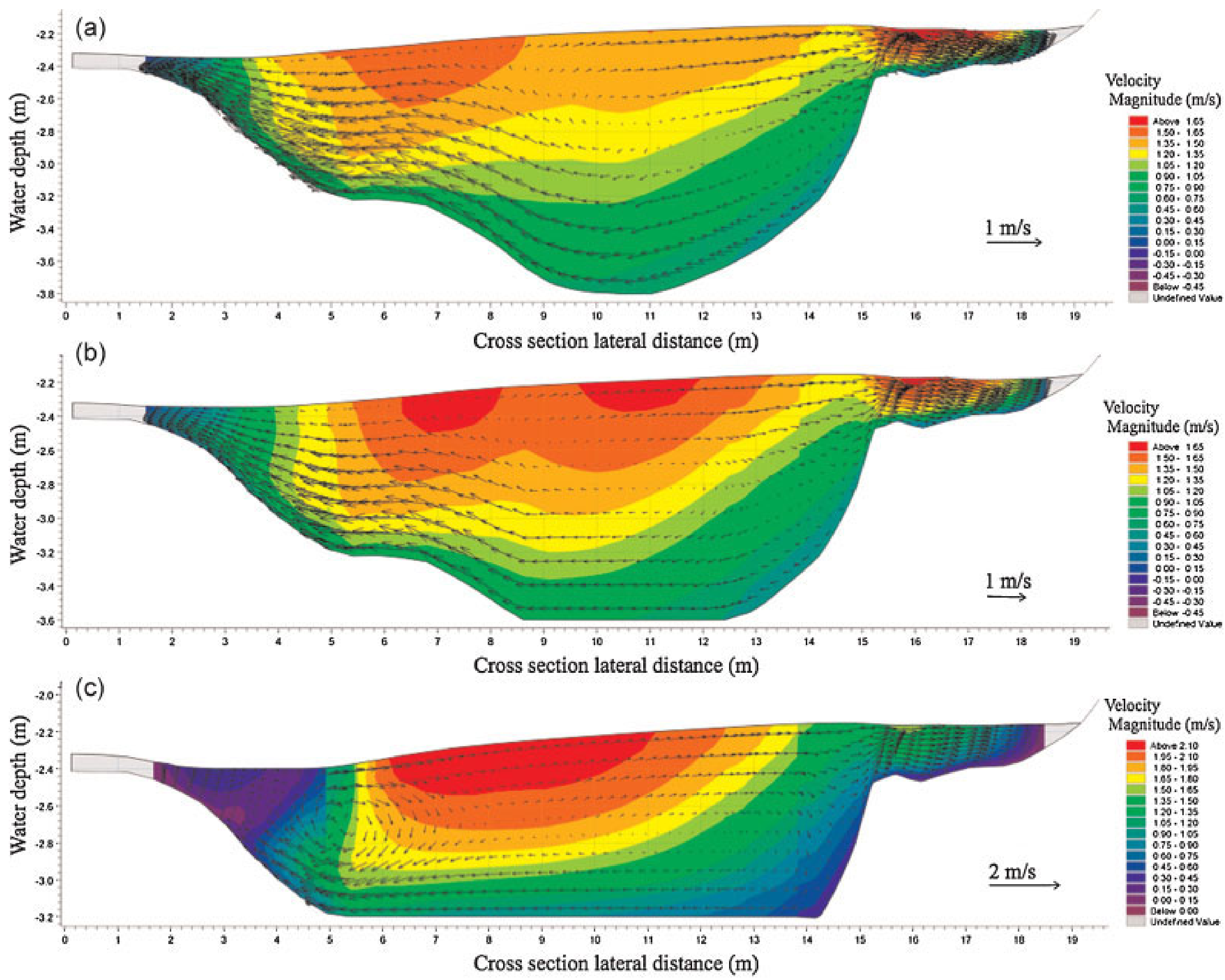

Figure 11. Predicted lateral velocity distribution in the upstream pool during the 16.63 m^3/s flow, with: a) 0%, b) 30% and c) 90% aggradation of residual depth. Vectors indicate patterns of secondary circulation. This figure is available in colour online at wileyonlinelibrary.com

CONCEPTUAL MODEL FOR SELF-FORMED POOL-RIFFLE SEQUENCES

Conceptual models offer an alternative to detailed site-specific modelling efforts (Rathburn and Wohl, 2003). Here, a conceptual model is proposed based on the analysis of the Red River site, which could be broadly applicable to other gravel-bed rivers with self-formed topography. The conceptual model provides a framework for expected flow structures and characteristics that can be used to guide monitoring of channel processes elsewhere. Based on detailed observations of the Red River site over the past 10 years since restoration and on the above flow simulations, the following characteristics can be postulated for the flow structure in self-formed pool-riffle features.

1. At any point in time, the flow structure is driven by the bathymetry. In pools, a jet is concentrated as the bar constricts the flow, regardless of whether the flow enters the pool from a riffle or run (Figures 8 and 9).
2. At different discharges, the alignment of the jet changes (Figures 8 and 9). At low discharges, the velocity through the deep part of the pool is reduced and this establishes a lateral pressure gradient that forces the jet towards the inner bank (Figure 9). However, as the discharge increases, the inertia of the jet becomes more important compared with the lateral pressure gradient, and at high discharge the jet follows the pool thalweg and is more closely aligned with the outer bank (Caamaño, 2008). The morphology of the study site has been essentially stable for the past 8 years and the effective discharge (that which transports the most sediment over time; Wolman and Miller, 1960) approximates the bankfull discharge in this reach (Klein *et al*., 2007). Therefore, the observation that the jet alignment moves from the inner bar towards

DOI: 10.1002/rra

the pool thalweg as flows approach the effective discharge is potentially significant, since it could thereby contribute to the sustainability of the pool; the jet would be positioned to scour the pool thalweg and maximize transport along it during the effective discharge.

3. The zone of jet concentration (run to pool or upstream riffle to pool) is followed by a zone of jet dissipation (pool to downstream riffle or pool to downstream run) (Figures 8–10). In the dissipation zone, the jet spreads across most of the riffle at all discharges and for both types of pool-riffle sequences studied. Following this zone of jet dissipation, another jet concentration zone may initiate downstream if the riffle is followed by another pool, or no jet concentration zone will be encountered if the riffle is followed by a run.
4. The jet flow drives large-scale turbulence features (Figures 8–11) that may be important for sediment transport and hydraulic sorting of bed material throughout the pool-riffle sequence (e.g. Dietrich and Smith, 1984; Parker and Andrews, 1985). There are also potentially important ramifications for aquatic habitat, as the eddies may serve as locations of velocity refugia at higher flows or as areas of drift food accumulation.
5. The dominant and most consistently observed turbulence structures are the horizontal eddies created on the inner banks downstream of riffles (Figure 8). These features extend over the entire water column. Vertical eddies persist on the outer banks at high flows and appear to have a role in directing the main jet flow away from the outer bank in stable pool features. These vertical eddies occur along a zone of flow separation, and they may reduce the effects of direct impingement of the jet on the outer bank for a pool that persists over time (Figure 9).
6. Secondary circulation is an important process for pool maintenance as this flow structure is responsible for building bars (Dietrich and Smith, 1984; Parker and Andrews, 1985). At discharges less than the effective discharge, the jet flow is expected to assist in building the bar, but at higher discharges the jet is aligned away from the bar towards the outer bank (Figure 8).
7. As the pool begins to fill with sediment (30% filling in this study), the jet is drawn away from the inner bar towards the pool at discharges that are lower than observed with the existing bathymetry (cf. Figures 9 and 11). This is a pool maintenance mechanism, as the high velocities and increased transport potential are moved back towards the pool thalweg, potentially allowing scour of previously deposited sediment (e.g. Gilbert, 1914, Keller, 1971, Lisle, 1979).
8. In contrast, if the pool continues to fill with sediment (90% filling in this study), the jet becomes wider and is also aligned more directly at the outer bank, increasing the likelihood of lateral bank erosion (Figures 10 and 11). The potential consequences of this are discussed below.

Based on these observations, a conceptual model for the sustainability of pool-riffle sequences can be postulated. Although primarily based on observations of the sustainability of pools at the study site during the 10 years following restoration, the postulations are consistent with elements of other observations (Dietrich and Smith, 1984, MacWilliams *et al*., 2006, Pasternack *et al*., 2008).

I. Pool aggradation or scour is a function of the difference between local transport capacity through the pool and sediment delivery from the upstream reach (e.g. Buffington *et al*., 2002). In most gravel-bed streams the transport is supply limited except during the highest flows when the armour layer breaks up (e.g. Milhous, 1973, Jackson and Beschta, 1982, Barry *et al*., 2004). So, the question is reduced to whether the transport through the pool is higher than the inflowing sediment at high flows, which will be achieved if velocity reversal and sediment transport reversal occur at some point as the discharge increases (e.g. Gilbert, 1914, Keller, 1971, Lisle, 1979).

II. Jet flow is concentrated by the constriction created by the alternate bars and it is this jet that defines the flow structure through the pool-riffle sequence. The characteristics of the jet flow likely govern the local transport capacity through the pool due to the higher near-bed velocities, and the jet is related to the horizontal and vertical eddy structures observed in this study and by other researchers (Richards, 2004, MacWilliams *et al*., 2006, MacVicar and Roy, 2007). These large-scale structures provide a measure of protection to the bank from the high velocities of the jet.

III. If the pool is deep, velocities are relatively low through the pool and energy considerations show that there is a lateral pressure gradient that moves the jet towards the inner bank and bar at low flows (Figure 9) (Dietrich *et al*., 1979; Dietrich and Smith, 1983). At higher flows (approaching bankfull), the inertia of the jet emanating from the run or upstream riffle becomes dominant, and the jet is forced towards the pool thalweg (Figure 9).

IV. If the inflowing sediment exceeds the transport capacity in the pool (Point I), the pool will gradually fill with sediment. The velocity distribution becomes more uniform across the section and the lateral pressure gradient becomes less significant, allowing the jet to pass through the pool thalweg at lesser discharges than occurs with the equilibrium pool condition with no aggradation (cf. Figures 9 and 11). If the pool aggradation becomes more significant, the jet alignment may cross the pool and impinge directly on the outer bank (Figures 10 and 11).

DOI: 10.1002/rra

V. If the outer bank is easier to erode than the channel bed (i.e. due to low bank strength or loss of riparian vegetation), it would be expected that the channel will maintain a wide shallow section, with little opportunity for the pools to scour back towards their original residual depths (Caamaño *et al*., 2009). Conversely, if the bank is resilient compared with the bed, and the sediment transport capacity through the pool is greater than the incoming sediment from upstream, the pool will scour back towards its original condition as the jet concentrates through the pool. In this situation, supply-limited gravel-bed streams will facilitate the pool recovery mechanism.

VI. As the pool deepens, the relative velocity through the pool thalweg decreases, again setting up the lateral pressure gradient, and the jet is forced back towards the inner bank at lower flows (Figure 8). The process of bar building due to the combined action of secondary currents and jet alignment reinforces this cycle that will sustain pool morphology (Richards, 2004).

SUMMARY

Three-dimensional hydraulic simulations and field observations for two self-formed pool-riffle sequences on a section of Red River, Idaho are analyzed. The predicted WSE and velocities agree well with the field observations, indicating that the model is well calibrated and that the numerical simulations are accurate. The model is used to visualize the spatial pattern of jets (or faster moving water in the cross section) through the study reach, with jets being defined as areas where velocities exceed 90% of the maximum depth-averaged velocity for a given cross section. Jet concentration and dissipation zones were observed within the pools at all three discharge scenarios (0.38, 5.67 and 9.23 m^3/s). Jets concentrate at the pool head and dissipate as water flows through the pool tail into the downstream riffle. The alignment of the jet is observed to change with discharge and bathymetry. Deeper pools show shorter, wider and faster jets with increasing discharge. Shallower pools generate jets that are relatively longer and increase in width at a slower rate than the same pools with a larger residual depth.

Detailed observation of the flow structure shows a relationship between the jet and macroscale turbulent features (vertical and horizontal eddies). The effect of pool aggradation on the jet characteristics and associated eddies is described. Finally the simulations and observations are combined into a conceptual model for pool sustainability. This proposed conceptual model seeks to explain the flow structure in pool-riffle morphology and how this flow structure will change as a result of altered external forcing, such as upstream sediment delivery or changes in bank stability. The insight provided by this model could assist stream managers in prioritizing actions that will improve pool sustainability without the need to create forced pool-riffle sequences by structural means, as is commonly done (e.g. Slaney and Zaldokas, 1997). Future work will compare the occurrence of velocity reversals determined from cross-sectional average parameters versus three-dimensional jet solutions.

ACKNOWLEDGEMENTS

Funding for this research was provided by the Chilean Government ‘‘Beca Presidente de la República para Estudios en el Extranjero’’, the DeVlieg Foundation and the University of Concepción, Chile. Additional support was provided by Congressional Award: Fund for the Improvement of Postsecondary Education (Award Number P116Z010107) Advanced Computing and Modeling Laboratory at the University of Idaho, the National Science Foundation Idaho EPSCoR Research Infrastructure Improvement (RII) Grant Grand Challenge Initiative, 2005-2008, the National Science Foundation under Award No. EPS-0447689 and DHI, Denmark. We thank the anonymous reviewers for comments that improved the manuscript.

REFERENCES

Barry JJ, Buffington JM, King JG. 2004. A general power equation for predicting bedload transport rates in gravel bed rivers. *Water Resources Research* **40**(10): W10401.

Booker DJ, Sear DA, Payne AJ. 2001. Modelling three-dimensional flow structures and patterns of boundary shear stress in a natural pool-riffle sequence. *Earth Surface Processes and Landforms* **26**(5): 553–576.

Buffington JM, Lisle TE, Woodsmith RD, Hilton S. 2002. Controls on the size and occurrence of pools in coarse-grained forest rivers. *River Research and Applications* **18**(6): 507–531.

Caamaño D. 2008. The velocity reversal hypothesis and implications to the sustainability of pool-riffle bed morphology. *PhD Dissertation*, Center for Ecohydraulics Research, University of Idaho, Boise.

Caamaño D, Goodwin P, Buffington JM, Liou JC, Daley-Larsen S. 2009. A unifying criterion for velocity reversal hypothesis in gravel-bed rivers. *Journal of Hydraulic Engineering* **135**(1): 66–70.

DHI. 2008. *MIKE 3 Flow Model FM*. Horsholm: Denmark.

Dietrich WE, Smith JD, Dunne T. 1979. Flow and sediment transport in a sand bedded meander. *Journal of Geology* **87**: 305–315.

Dietrich WE, Smith JD. 1983. Influence of the point bar on flow through curved channels. *Water Resources Research* **19**: 1173–1192.

Dietrich WE, Smith JD. 1984. Bed load transport in a river meander. *Water Resources Research* **20**(10): 1355–1380.

Gilbert GK. 1914. The transportation of Débris by Running Water. U.S. Geological Survey Professional Paper 86.

Goodwin P. 2004. Analitical solutions for estimating effective discharge. *Journal of Hydraulic Engineering* **130**(8): 729–738.

DOI: 10.1002/rra

Gunawan B, Sterling M, Knight DM. 2009. Using an acoustic Doppler current profiler in a small river. *Water and Environment Journal.* Published online 12 May 2009 DOI: 10.1111/j. 1747-6593. 2009.00170.x.

Harrison LR, Keller EA. 2007. Modeling forced pool-riffle hydraulics in a boulder-bed stream, southern California. *Geomorphology* **83**(3–4): 232–248.

Jackson WL, Beschta RL. 1982. A model of two-phase bedload transport in an Oregon Coast Range stream. *Earth Surface Processes and Landforms* **7**: 517–527.

Jirka GH. 2007. Buoyant surface discharges into water bodies. II: Jet integral model. *Journal of Hydraulic Engineering* **133**(9): 1021–1036.

Keller EA. 1971. Areal sorting of bed-load material: the hypothesis of velocity reversal. *Bulletin of the Geological Society of America* **82**(3): 753–756.

Klein LR, Clayton SR, Alldredge JR, Goodwin P. 2007. Long-term monitoring and evaluation of the lower Red River meadow restoration project, Idaho, USA. *Restoration Ecology* **15**(2): 223–239.

Lamb MP, Dietrich WE, Venditti JG. 2008. Is the critical Shields stress for incipient-sediment motion dependent on channel-bed slope? *Journal of Geophysical Research Earth Surface* **113**: FO2008.

Lisle T. 1979. A sorting mechanism for a riffle-pool sequence. *Geological Society of America Bulletin* **90**(II): 1142–1157.

Lisle TE. 1987. *Using residual depths to monitor pool depths independently from discharge*, USDA Forest Service Research Note PSW-394. Pacific Southwest Research Station: Albany, CA.

MacVicar BJ, Roy AG. 2007. Hydrodynamics of a forced riffle pool in a gravel bed river: 1. Mean velocity and turbulence intensity. *Water Resources Research* **43**: W12401.

MacWilliams ML, Wheaton JM, Pasternack GB, Street RL, Kitanidis PK. 2006. Flow convergence routing hypothesis for pool-riffle maintenance in alluvial rivers. *Water Resources Research* **42**: W10427.

Milhous RT. 1973. Sediment transport in a gravel-bottomed stream. *Ph.D. Dissertation*, Oregon State University: Corvallis.

Montgomery DR, Buffington JM, Smith RD, Schmidt KM, Pess G. 1995. Pool spacing in forest channels. *Water Resources Research* **31**(4): 1097–1105.

Parker G, Andrews ED. 1985. Sorting of bed load sediment by flow in meander bends. *Water Resources Research* **21**(9): 1361–1373.

Pasternack GB, Bounrisavong MK, Parikh KK. 2008. Backwater control on riffle-pool hydraulics, fish habitat quality, and sediment transport regime in gravel-bed rivers. *Journal of Hydrology* **357**(1–2): 125–139.

Phillips NA. 1957. A coordinate system having some special advantages for numerical forecasting. *Journal of the Atmospheric Sciences* **14**(2): 184–185.

Rathburn S, Wohl E. 2003. Predicting fine sediment dynamics along a pool-riffle mountain channel. *Geomorphology* **55**(1–4): 111–124.

Richards KS. 2004. *Rivers: Form and Process in Alluvial Channel*. The Blackburn Press: Caldwell, New Jersey.

Rodi W. 1984. *Turbulence models and their applications in hydraulics*. A state of art review. International Association for Hydraulics: Research, Delft, Netherlands.

Slaney PA, Zaldokas D. editors. 1997. *Fish habitat rehabilitation procedures*, Watershed Restoration Technical Circular No. 9. Ministry of Environment, Lands, and Parks: Vancouver, British Columbia, Canada.

Smagorinsky J. 1963. General circulation experiments with the primitive equations. *Monthly Weather Review* **91**: 99–164.

Tonina D, Buffington JM. 2007. Hyporheic exchange in gravel-bed rivers with pool-riffle morphology: Laboratory experiments and three-dimensional modeling. *Water Resources Research* **43**(1): W01421.

Tritton DJ. 1977. *Physical Fluid Dynamics*. Van Nostrand Reinhold Company: New York.

Wiberg PL, Smith JD. 1991. Velocity distribution and bed roughness in high-gradient streams. *Water Resources Research* **27**(5): 825–838.

Wolman MG. 1954. A method of sampling coarse river-bed material. *Transactions of the American Geophysical Union* **35**(6): 951–956.

Wolman MG, Miller JP. 1960. Magnitude and frequency of forces in geomorphic processes. *Journal of Geology* **68**: 54–74.

DOI: 10.1002/rra